New formamidine ligands and their mixed ligand palladium(II) oxalate complexes: Synthesis, characterization, DFT calculations and in vitro cytotoxicity

Ahmed A. Soliman, Othman I. Alajrawy, Fawzy A. Attabi, Mohamed R. Shaaban, W. Linert

PII: S1386-1425(15)30125-6
DOI: http://dx.doi.org/10.1016/j.saa.2015.07.076
Reference: SAA 13975

To appear in: *Spectrochimica Acta Part A: Molecular and Biomolecular Spectroscopy*

Received Date: 17 April 2015
Revised Date: 19 June 2015
Accepted Date: 16 July 2015

Please cite this article as: A.A. Soliman, O.I. Alajrawy, F.A. Attabi, M.R. Shaaban, W. Linert, New formamidine ligands and their mixed ligand palladium(II) oxalate complexes: Synthesis, characterization, DFT calculations and in vitro cytotoxicity, *Spectrochimica Acta Part A: Molecular and Biomolecular Spectroscopy* (2015), doi: http://dx.doi.org/10.1016/j.saa.2015.07.076

New formamidine ligands and their mixed ligand palladium(II) oxalate complexes: Synthesis, characterization, DFT calculations and in vitro cytotoxicity

Ahmed A. Soliman[1*], Othman I. Alajrawy[1, 2], Fawzy A. Attabi[1] , Mohamed R. Shaaban[1] and W. Linert[3]

[1]Department of Chemistry, Faculty of Science, Cairo University, 12613 Giza, Egypt.
[2]College of Veterinary Medicine, Al-Anbar University, Fallujah, Iraq
[3]Institute of Applied Synthetic Chemistry, Vienna University of Technology, Getreidemarkt 9163-AC, A-1060 Vienna, Austria.

Abstract

A series of new ternary palladium(II) complexes of the type $[Pd(L_{1-4})ox].xH_2O$ where L= formamidine ligands and ox=oxalate, were synthesized and characterized by elemental analyses, magnetic susceptibility, UV-Vis, infrared (*IR*) and mass spectroscopy and thermal analysis. The spectroscopic data indicated that the formamidine ligands act as bidentate N2 donors and the oxalate as O2 ligand. The complexes (**1-4**) are diamagnetic and the optimization of their structures indicated that the geometry is distorted square planer with O-Pd-O and N-Pd-N bond angles ranged 82.70°-83.87° and 88.21°-95.02°; respectively which is acceptable for the heteroleptic complexes. The dipole moment of the complexes (13.97-18.77 Debye) indicating that the complexes are more polarized than the ligands (1.93-4.96 Debye). The complexes are thermally stable as shown from their relatively higher overall activation energies (441-688 $kJmol^{-1}$). The ligands and the complexes are proved to have good cytotoxicity with IC_{50} (μM) in the range of (0.011-0.168) against MCF-7, (0.012-0.150) against HCT-116, (0.042-0.094) against PC-3 and (0.006-0.222) against HepG-2 cell lines, which open the field for further application as antitumor compounds.

Keywords: ternary Pd(II) complexes, oxalate, formamidine, antitumor complexes.

*Correspondent author: Prof. Dr. Ahmed A Soliman, e-mail: ahmedsoliman61@gmail.com, Tel: 002 01110121379, Fax: 002 02 35676556.

1. INTRODUCTION

Over decades, pharmaceutical chemistry of anticancer drugs has been extensively reported with the aim of design and test new anticancer drugs, potentially valuable in the treatment of a lot of cancers [1-4]. The preparation of novel highly cytotoxic active both platinum and non-platinum coordination compounds successfully use a combination of potentially active organic compounds with a suitable transition metal [5]. Plenty of transition metal complexes, namely iron(II/III), cobalt(II), nickel(II), copper(II), zinc(II), ruthenium(III), palladium(II), platinum(II) and platinum(IV) [5], have been prepared, characterized and tested *in vitro* for their cytotoxic activity against selected human cancer cell lines. Oxaliplatin is the most important representative of platinum(II) oxalate complexes[6], because it belongs among the recently used platinum-based anticancer drugs (approved in 1996) [4, 7]. The elements of platinum and palladium are chemically very similar, that is why palladium complexes were tested for their cytotoxicity among the first non-platinum compounds. However, *cis*-$[PdCl_2(NH_3)_2]$ and $[PdCl_2(dach)]$ the analogues of the highly cytotoxic platinum(II) complexes, were found to be inactive on a Sarcoma 180 tumor cell line [8]. Generally, the lower efficiency of palladium (II) complexes than the platinum (II) analogues is attributed to the fact that palladium (II) complexes are of about 10^5 times faster substitution of the leaving groups for the water molecules. Despite these early failures, plenty of palladium complexes have been prepared to date and many of these compounds were evaluated as substances with even higher cytotoxic activity against various types of tumors as compared with ***cisplatin*** [7, 9].

On the other hand and up to the best of our knowledge, there are no reports on the metal complexes of the used formamidine ligands except the study conducted in our group on the binary complexes of palladium (II) and ruthenium(II) were prepared and investigated [10]. In view of the above facts, it seems therefore to be of considerable interest to conduct investigations of ternary complexes of palladium (II) with some formamidines and oxalate ligands as potential antitumor complexes. In continuation of our published work on palladium complexes [10, 11], we report in the present synthesis, characterization, structure optimization and antitumor activity of palladium complexes of formamidine [10] and oxalate ligands. The formamidine ligands are given in **Scheme 1**.

2. Experimental.

2.1. Materials.

All chemicals used in this study were of the highest purity available. Sodium tetrachloropalladate(II), $Na_2[PdCl_4]$ and potassium oxalate monohydrate, $K_2C_2O_4.H_2O$ were supplied by Aldrich. All solvents were of analytical grade and were purified by distillation before use.

2.2. Measurements.

Infrared measurements of the solid complexes, as KBr pellets, were carried out using Jasco FTIR-460 plus and Jasco FTIR-4000 (range 400-4000 cm^{-1}), mass spectrometry measurements were carried out using GCMS-QP1000EX Shimadzu. The magnetic susceptibility of the complexes in the solid state was carried out using a Sherwood Scientific, Cambridge Science Park Cambridge-England magnetic susceptibility balance. Thermal analysis of the complexes were carried out using a Shimadzu thermo-gravimetric analyzer TGA-60H; under a nitrogen atmosphere with a heating rate of 10 ^oC /min over a temperature range from room temperature up to 1000 ^oC. UV-Vis spectra were recorded in a 1 cm path length quartz cell by using optizen UV-Vis spectrophotometer.

2.3. Preparation of complexes

$K_2[Pd(ox)_2].2H_2O$ was synthesized using a slightly modified and previously published procedure[12] and stored in dark and cold place throughout the study. Both sodium tetrachloropalladate(II); Na_2PdCl_4, and potassium oxalate monohydrate; $K_2C_2O_4.H_2O$, were dissolved separately in a minimum volume of distilled water, at 25 ^oC, in a 1:2 (Pd: ox) molar ratio. 1 mmol of $\mathbf{L_1}$(0.21 g), $\mathbf{L_2}$(0.19 g), $\mathbf{L_3}$(0.14 g) or $\mathbf{L_4}$(0.12 g) was dissolved in 10 mL of ethanol and slightly added to a water solution (10 mL) of 1 mmol (0.40 g) $K_2[Pd(ox)_2].2H_2O$. The mixtures were stirred for 24 h at 40 ^oC. The obtained yellow solids complexes $[Pd(L_1)(ox)].H_2O$ (**1**) (0.312 g; yield: 74.2%), $[Pd(L_2)(ox)].H_2O$ (**2**) (0.289 g; yield: 72.2%), $[Pd(L_4)(ox)].5/2H_2O$ (**4**) (0.272 g; yield: 74.9%), and yellow-orange $[Pd(L_3)(ox)].4H_2O$ (**3**) (0.301 g; yield: 73.9%), ternary complexes were filtered off, washed with warm water, ethanol and dried in vacuum dissector. Geometric parameters and energies of prepared complexes were

carried out using [GAUSSIAN 09W] software program. Molecular geometry of the singlet ground state of complexes was fully optimized in the gas phase at the B3LYP level of theory.

3. Results and discussion

The analytical, physical and UV-Vis spectroscopic data of the ligands and their isolated metal complexes are given in Table 1. The complexes are air stable and exhibit very poor solubility in all solvents except DMSO in which complexes (**1**), (**2**) and (**4**) are soluble while (**3**) is not.

3.1. IR Spectra.

The IR spectra of the complexes were compared with those of the free ligands (L_1-L_4, ox) in order to monitor the change in the vibration frequency of the coordination sites, which may be involved in chelation. The characteristic peaks of all ligands and its complexes are listed in Table 2. The IR spectra of the free ligands showed a strong band at 1600-1640 cm^{-1} assignable to ν(C=N) of the azomethine and a weak band at 1261-1276 cm^{-1} assignable to ν(C-N) [13]. The IR spectra of complexes (**1-4)** showed strong bands at 1627-1641 cm^{-1} to ν(C=N) of the azomethine and new bands at 1699-1712 cm^{-1} due to ν(C=O). Furthermore, in all cases, the infrared spectra showed the typical patterns of dicarboxylate ligands bound in a bidentate fashion to a metal center with shoulder of ν(COO^-) in the range 1310-1400 cm^{-1} [14, 15]. Figure 1 shows the calculated and experimental IR spectra of the complex 1 as representative example**.** The calculated IR data are in good agreement with the experimental ones (Table 2). The relative error is in the range (0.1-6.2%). The small deviation in the calculated vibrations may attributed to the fact that the computed wavenumbers are corresponded to the isolated molecular state, whereas the observed wavenumbers correspond to the solid state spectra;

3.2. Mass spectral analysis.

The mass spectral data of the complexes showing the major mass fragmentation peaks are listed in Table 3. Mass spectrum of complex (**1**) (molecular weight equals 418) gave a parent peak at m/z = 420 (M+2), a peak at m/z =402 assigned for (M+2-H_2O) , a peak at m/z =334 assigned for (M+2-C_2O_4), a peak at m/z =215 assigned for (M^+-L_1), a peak at m/z =205 assigned for (L_1). The mass spectrum of complex (2) (molecular weight equals 400.68), gave a parent peak at m/z = 400 (M^+), a peak at m/z =382 assigned for (M^+-H_2O) , a peak at m/z =307

assigned for (M^+-C_2O_4)a peak at m/z =213 assigned for [M^+-L_2)] , and a peak at m/z =184 assigned for (L_2). Mass spectrum of complex (**3**) (molecular weight equals 407), gave a parent peak at m/z=408 (M+2), a peak at m/z=339 assigned for (M+2-4H_2O), a peak at m/z=326 assigned for (M+2-C_2O_4), a peak at m/z=264 assigned for (M+2-L_3), and a peak at m/z=139 assigned for (L_3). The mass spectrum of complex (**4**) (molecular weight equals 361), gave a parent peak at m/z = 363 (M+2), a peak at m/z =315 assigned for (M+2-5/2H_2O), a peak at m/z =273 assigned for [M+2- C_2O_4] , a peak at m/z =238 assigned for [M+2-L_4] and a peak at m/z =121 assigned for (L_4), indicate that all complexes are separated as monomers associated with at least one uncoordinated water molecule. It is interesting also to highlight the contribution of the different isotopes of palladium to the molecular mass of complexes. The mass spectra of the complexes showed the stable palladium isotopes peaks at 104, 105,106, 108 and 110 [16].

3.3. Electronic Spectra.

The electronic spectral data of the DMSO solutions of the free ligands, recorded in the 200 – 1100 nm are given in Table 1. The complexes (1, 2, 4) exhibited absorption bands in the range 300–340 nm and 340–400 assigned to the $\pi\rightarrow\pi^*$ and $n\rightarrow\pi^*$ transitions; respectively, of benzene ring and the azomethine group respectively [11]. The spectra showed also shoulders at 400-420 nm which may be assigned to MLCT (metal to ligand charge transfer) within a square planar moieties [17, 18]. It is worthy to mention that complex (**3**) is insoluble. The values of the experimental absorption peaks were compared with the computed excitation energies (eV). The computed main excitation, electronic transition configurations and oscillator strength of Pd complexes are given in Table 4. The calculated electronic transitions for the complexes (**1, 2, 4**) were of good agreement with the experimental values; Table 4 and **Fig**. 2. The assignment of the calculated orbital excitations to the experimental bands was based on the relative energy of the HOMO and LUMO orbitals involved in the electronic transitions which provides a better estimation of excitation energies and oscillators strengths, especially for transitions with charge-transfer character.

3.4. Magnetic Susceptibility Measurements.

Measurements of the magnetic susceptibility of palladium complexes (1-4) in the solid state showed that they are diamagnetic. The diamagnetism of the complexes can be explained on the fact that Pd(II) (with d^8 configuration) in a square planner geometry may have the electronic distribution $eg^4\ a_{1g}{}^2\ b_{2g}{}^2$ with all electrons paired [19].

3.5. Thermal Analysis.

The thermal studies of the complexes were carried out using the thermogravimetric analysis (TGA) and the derivative thermogravimetric analysis (DrTGA) to investigate the thermal stability of the complexes and the type and number of water associated with the complexes. The complexes decomposed in three to five steps and ended with Pd metal as the metallic residue, Table 4. The decomposition of the complexes is consistent with the proposed formulae. Calculation of thermodynamic parameters using Integral method using the Coats–Redfern and Approximation method using Horowitz–Metzger [20,21]. The temperature ranges of decompositions along with the corresponding mass loss of species are given in Tables 5. A typical TGA and DrTGA plots for complexes (**1**) and (**3**) as representative example is shown in Fig. 3. All thermodynamic parameters of the four complexes are given in Table 6. The complexes showed high thermal stability which is reflected from the relatively higher overall activation energies (441-688 $kJmol^{-1}$). The entropy change, ΔS^*, of the formation of the activated complexes from the starting reactants varied from positive to negative values within the decomposition steps. This variation in the sign of the entropy change from a decomposition step to another one consistent with the variation in the degree of structural 'complexity' (arrangement, 'organization') of the activated complex as the starting reactants are different [22-24].

3.6. Computational Studies

In the absence of a crystal structure and to obtain the molecular conformation of the complexes (**1-4**), energy minimization studies were carried out using GAUSSIAN 09W software program (institutional copy of the Faculty of Science, Cairo University). Molecular geometries of the singlet ground state of complexes were fully optimized in the gas phase at the B3LYP level of theory. The SDD basis set for all atoms was employed in the calculations [25, 26]. The optimized geometries of the complexes are given in ***Scheme 2***. Selected bond lengths and angles

are given in Table 7. A comparison of the calculated Pd-O and Pd-N bond lengths with those of reported palladium(II) oxalato complexes involving bidentate *N*-donor ligands, whose average values were found to be for Pd-O; (1.999-2.105 Å) range is consistent with the range of values reported for five and six-membered chelates containing Pd-O bonds [27-29], and for Pd–N; (2.03-2.09 Å) range [30-32], indicated that the mentioned parameters correlate well in the case of the Pd-O bonds. The angles around central metal ion Pd(II) with surrounded four atoms of two ligands vary from 82.70° to 96.64°, these values deviated from those expected square planar indicating that structures are distorted square planar [33]. The O-Pd-O bond angles whose average values were found to be (82.70°-83.87°) within the chelating ring is comparable with the other palladium(II) carboxylato complex, e.g. 82° in $K_2[Pd(C_2O_4)_2].4H2O$ [34] and 81.1° in oxalate cis-bis(triethylphosphine)palladium(II) [35]. The N-Pd-N bond angles whose average values were found to (88.21 °-95.02 °) are deviating from the ideal value (90^o). This may be attributed to bulky nature of the ligand. The slight deviations in both bond lengths and bond angles may be attributed to the nature of complexes (**1-4**) as heteroleptic formed by two different ligand with two different groups of donor atoms (N2 and O2) while the reported complexes used in comparison are homoleptic.

The calculation of atomic charges is a very important parameter that is used in the application of quantum mechanical calculation to describe the electronic characteristics of molecular system [29]. The charge densities were found on nitrogen atoms of all ligands in the range (-0.060)-(-0.151); Scheme ***1***. This indicates that the suitability of the nitrogen atoms (L_1-L_4) for coordination to the positively charged palladium. The positive charge on sulfur atom in $\mathbf{L_1}$ (0.249) and in complex (**1**) (0.376) omits the possibility of sulfur as binding site. It has been found that in the four complexes, the charges on the coordinated nitrogen atoms are increased to the range (-0.273)-(-0.338) which indicates the back donation from the metal sites in a MLCT mode to the π* orbitals of the ligand. The distribution of the atomic charges is also important in the determination of the direction of the dipole moment vector in the complexes which depends on the centers of negative and positive charges.

The dipole moment and the electronic energies of the ligands as well as complexes are given in Table 8 . The dipole moment of the complexes (13.97-18.77 Debye) indicating that the complexes are more polarized than the ligands (1.93-4.96 Debye). The electronic energies (a.u.) of the complexes (- 902. 09 to -1455.04) and that of the ligands (-397.04- 949.99) indicate their stability. The calculated energies of the highest occupied molecular orbital (HOMO) and the

lowest unoccupied molecular orbital (LUMO) of the ligands (**L_1-L_4**) and their palladium (II) complexes (**1-4**) are listed in Table 8. The hardness (η) is defined as (η= (*I-A*)/2) where I is the ionization energy and A is the electron affinity. On the other hand, the (*I-A)* equals the gap between the HOMO and LUMO. Hence, the hardness of the present ligands and complexes can be calculated as ((η= (E_{HOMO}-E_{LUMO})/2). Hard molecules have high the HOMO-LUMO gap, and soft molecules have smaller HOMO-LUMO gap [36, 37]. The values η and ΔE (HOMO-LUMO) are given in Table 8. It is obvious from the table that the complexes are soft (η= (0.046-0.054), where for ligands (η=0.053-0.155). It is also that the electronic transition within the complexes is easy as indicated from the ΔE of complexes (0.092-0.108), where for ligands (0.106-0.310).

The frontier molecular orbitals (FMOs) can offer reasonable qualitative indication of the excitation properties and the electron transport. The energies of the HOMO and LUMO orbitals of the ligands and their complexes were negative which indicates that the ligands and the complexes are stable compounds, the values of HOMO and LUMO orbitals and their energy gap reflect also the chemical activity of the molecule [38]. The values of the energy separation between the HOMO and LUMO for complexes (1-4) are in agreement with the values for stable transition metal complexes [28, 39]. Figure 4 shows the isodensity surface plots of HOMO and LUMO for **L_1** and complex (**1**); as example, the electron density of HOMO and LUMO in **L_1** are mainly localized on the benzthoizole part of the ligand and the electronic transition could be described as a mixed π→π* and n→π* transition. The energies of HOMO sates (H to H-4), the % contribution and the main characters of Pd, oxalate (Ox) and formamidine ligand (**L_1-L_4**) in complexes (**1-4**) are calculated and given in Table 8. The % contribution of Oxalate (Ox) to the different HOMO states in Complex (**1**) varies from 34% to 95% and the main character is Ox (π). The % Contribution of Oxalate to different LUMO states (L to L+4) is much lower (0%-71%). The % contribution of **L_1** (complex (**1**)) in the different HOMO are low and varies from 1% to 18% through **L_1**(π) as the main character while the % contribution to LUMO states are much higher and varies from 29% to 90% through **L_1**(π*) as the main character. It is obvious from Table 8 that Ox has higher contribution to the different HOMO states than L1 which has on contrary higher contribution to the LUMO states. Therefore the π–π* electronic transition within the complexes may be arose from the transition from HOMO states of high Ox(p) character to LUMO states of **L_1**(π*) character. The % contribution of Pd to the HOMO states varies from 5%

to 33% by Pd(t_{2g}) as the main character except H-3 which 61% contribution through Pd(eg) which gives rise to the possibility of MLCT from Pd(eg) to either Ox(π*) and/or $\mathbf{L_1}$(π*). On the other hand, the % contribution of Pd to the LUMO states varies from 1% to 7% except L+1 in which the contribution of Pd is 48% which points to the possibility of LMCT from Ox(π*) and/or $\mathbf{L_1}$(π*) to Pd(eg) [17]. The % contribution and the main characters of Pd , oxalate (Ox) and formamidine ligand ($\mathbf{L_2}$-$\mathbf{L_4}$) to the different HOMO and LUMO states in complexes (**2-4**) showed more or less the same trend as complex(**1**).

The molecular electrostatic potential (MEP) is used for predicting sites and relative reactivity towards electrophilic and nucleophilic attack. The negative (red) regions of the MEP are related to electrophilic reactivity and the positive (blue) regions of nucleophilic reactivity. For the free ligands $\mathbf{L_1}$-$\mathbf{L_4}$ (Fig.5) the negative (red) regions are mainly localized over the nitrogen atoms of the ligands and hence it would be predicted that the nitrogen atoms will be the most reactive sites for electrophilic attack. In complexes, the negative (red) regions are mainly localized over the carbonyl- oxygen atoms of the coordinated oxalate ligand (Fig.6).

3.7. In vitro cytotoxic

In vitro cytotoxic activities of the formamidine ligands ($\mathbf{L_1}$-$\mathbf{L_4}$) and their mixed ligand complexes (**1, 2,** and **4**) were tested against the, human breast adenocarcinoma (MCF-7), liver carcinoma cell line (HEPG-2), and colon carcinoma cell line (HTC-116). For the evaluation of the IC50, the cell lines (100 µL each) were incubated for 48 h with various concentrations of the complexes, ranging from 0 to 100 µg/mL (100 µL volume) using doxorubicin as reference. As the total volume of the well was 200 µL, the concentration was taken as the number of micromoles (µM) were calculated from the micrograms of the complex. The complexes showed higher cytotoxicity against MCF-7 and HCT-116 compared with HEPG-2 as inferred from their %inhibition (Table 9). The IC_{50} values (µM) of the three tested complexes were compared with the doxorubicin as reference; Table 10. In general the ligands as well as their Pd(II) complexes have good IC_{50} values and the ligand $\mathbf{L_1}$-$\mathbf{L_4}$ has relatively lower IC_{50} values than those of the complexes which may be attributed the bulkiness and limited solubility of complexes. $\mathbf{L_4}$ being the simplest ligand has the lower IC_{50} with high potential to be applied as antitumor reagent.

Conclusion

Based on the spectroscopic, magnetic, thermal and theoretical data; the complexes (**1-4**) have distorted square planer geometry in which the formamidine ligands act as bidentate N2 donors and oxalate as bidentate O2 ligand. The distortion is indicated from the deviation of the O-Pd-O and N-Pd-N angles from 90^{o}. The distortion may be attributed to the heteroleptic nature of the complexes with two different coordinated ligands. The energies of the HOMO and LUMO orbitals of the ligands and their complexes were negative which indicates that the ligands and the complexes are stable compounds. The complexes are thermally stable as shown from their the relatively higher overall activation energies (441-688 $kJmol^{-1}$). The ligands and complexes are proved to have good cytotoxicity against some tumor cell lines which open the field for further application as antitumor compounds.

References

[1]. C. Orvig, M. Abrams, Chem. Rev. 99 (1999) 2201- 2204.

[2]. I. Warad ,A. F. Eftaiha, M. A. Al-Nuri 1, A. I. Husein 1, M. Assal, A. Abu-Obaid, N. Al-Zaqri, T. B. Hadda, B. Hammouti. J. Mater. Environ. Sci. 4 (4) (2013) 542-557.

[3]. B. Rosenberg, L. Van Camp and T. Krigas, Nature 205 (1965) 698–699.

[4]. L.R. Kelland, and N.P.Farrell, Platinum-Based Drugs in Cancer Therapy, Humana:Totowa, 2000.

[5] Z. Trávníček, I. Popa, M. Čajan, R. Zbořil, V. Kryštof and J. Mikulík, J. Inorg. Biochem. 104 (2010) 405–417.

[6]. Y. Kidani, K.Inagaki, M.Iigo, A.Hoshi and K.Kuretani, J.Med. Chem. 21 (1978) 1315–1318.

[7]. M. Gielen and E.R.T. Tiekink, Metallotherapeutic Drugs and Metal-based Diagnostic Agents, Willey: London, 2005.

[8]. J.L. Butour, S.Wimmer, F.Wimmer and P. Castan, Chem. Biol. Interact.104 (1997)165 178.

[9]. A. Garoufis, S.K. Hadjikakou, N. Hadjiliadis, Coord. Chem. Rev. 253(2009), 1384–1397.

[10]. A. M**.** Sayed, Synthesis, characterization and antitumor activity of palladium complexes with some new formamidine ligands, M.Sc. Thesis, faculty of science, Cairo university, 2013.

[11]. [11]. S. R. Majeed, analytical and inorganic studies of new antitumor palladium (II), ruthenium (II) and platinum (IV) complexes, PhD. Thesis, faculty of science, Cairo university, 2013.

[12]. P. Štarha, Z.K. Trávnícek , I. Popa, J. Inorg. Biochem. 103 (2009) 978–988.

[13]. N. Nakamoto, Infrared and Raman Spectra of Inorganic and Coordination Compounds, Wiley, New York, 1986.

[14]. S.R. Ali Khan, I.Guzman-Jimenez, K.H. Whitmire, A.R. Khokhar, Polyhedron 19 (2000) 983.

[15]. J. D. Hoeschel, Oak Ridge, Tenn.; Alan R. Amundsen, Somerville, NJ. : Engelhard Minerals & Chemicals Corp., Iselin, NJ. 106,439, 26, 1979

[16]. R. P. Bush, Recovery Of Platinum Group Metals From High Level Radioactive Waste Possibilities Of Separation And Use Re-Evaluated, Platinum Metals Rev., 1991, 35, (4), 202-208

[17]. A. B. P. Lever "Inorganic electronic spectroscopy", Elsevier, Amsterdam, 2nd ed, (1984) 544.

[18]. G. C. Pellacani, W. D. D. Malavasi, J. Inorg. Nucl. Chem. 37 (197 5)477-481.

[19]. Housecroft C. E., Sharpe A. G.. Inorganic Chemistry, 2nd ed, England, Pearson,2005, p. 579.

[20]. H. H. Horowitz, G. Metzger, Anal. Chem., 35 (1963) 1464-1468.

[21]. A. W. Coats, J. P. Redfern, Nature, 201 (1964) 68-69.

[22]. Soliman A. A., Samir M. E. and Omyma A. M. Ali, Thermal study of chromium and molybdenum complexes with some nitrogen and nitrogen-oxygen donors ligands, J. Thermal. Anal. &Cal., 2006;83(2):385-92.

[23]. A. A. Soliman, M. M. Khattab, R. M. Ramadan, Transit. Met. Chem., 32, 331(2007).

[24]. S.A. Ali, A.A. Soliman, M.M. Aboli, R.M. Ramadan, J. Coord. Chem. 55 (2002) 1161–1170.

[25]. T. H. Dunning Jr., P. J. Hay, *Modern Theoretical Chemistry*, 3rd Ed., Vol. 3, Plenum, New York, 1976, pp. 1–28.

[26]. D. Andrae, U. Häußermann, M. Dolg, H. Stoll, H. Preuß, *Theor. Chem. Acc.* 77 (1990) 123

[27]. Marwa G. Elghalban, Ahmed M. El Defarwy, Reem K. Shah, Mohamed A. Morsi, Int. J. Electrochem. *Sci.,* 9 (2014) 2379 – 2396.

[28]. Xavier Assfeld, J.L. Rivail, *Chem. Phys. Lett.* 263 (1996) 100–106.

[29]. A. M. Mansour, Inorganica Chimica Acta 394 (2013) 436–445.

[30]. Sadeek A. Sadeek, Walaa H. El-Shwiniy, Wael A. Zordok1 and Akram M. El-Didamony, The Journal of the Argentine Chemical Society Vol. **97** N° 2, 128-148 (2009).

[31]. A. K. Singh, J. Sooriyakumar, S. Husebye, K. W. Tornroos, *J. Organomet. Chem.* 612 (2000) 46.

[32]. D. R. Billodeaux, F. R. Fronczek, A. Yoneda, G. R. Newkome, *Acta Crystallogr. C* C54 (1998) 1439.

[33] M. Kaplun, M. Sandström, D. Boström, A. Shchukarev, P. Peresson, *Inorg. Chim. Acta* 358 (2005) 527.

[34]. D. J. Robinson, C. H. L. Kennard, *J. Chem. Soc. A* (1970) 1008.

[35]. X.-M. Luo, X.-H. Chen, S. Shanmuga Sundara Raj, H.-K. Fun, L.-G. Zhu, *Acta Crystallogr. C* 55 (1999) 1220.

[36]. K. Krogmann, Z. Anorg. Allg. Chem., 346, 188 (1966).

[37]. A.L. Rheingold, S. Yollies, R.M. Roat, W.C. Fultz and S.A. Kretchmar, Acta Crystallogr. Sect. C (Cr. Str. Comm), 43, 167(1987).

[38]. J.G. Małecki , P. Zwolinski, Polyhedron 39 (2012) 85–90.

[39]. **Pavel Štarha, Igor Popa and Zden k Trávní ek,** *Molecules 19*, 2014, 3832-3847. doi:10.3390/molecules19033832.

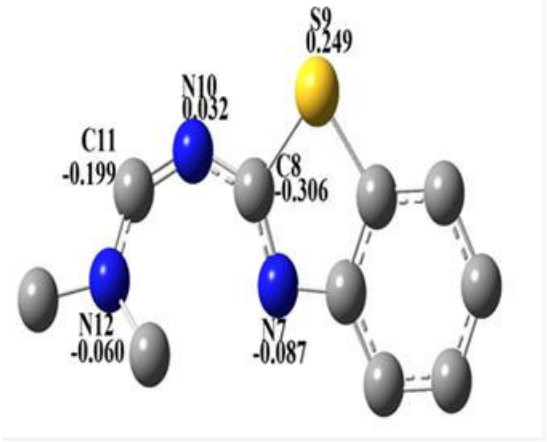

L_1

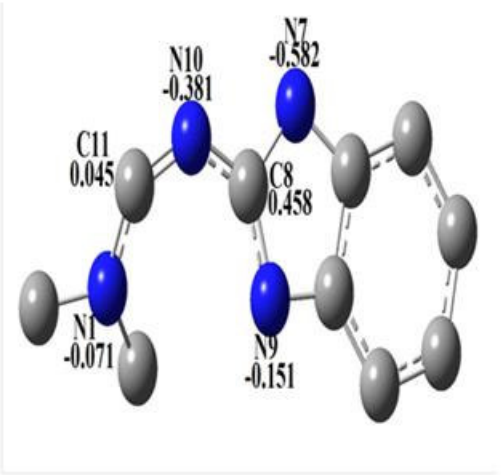

L_2

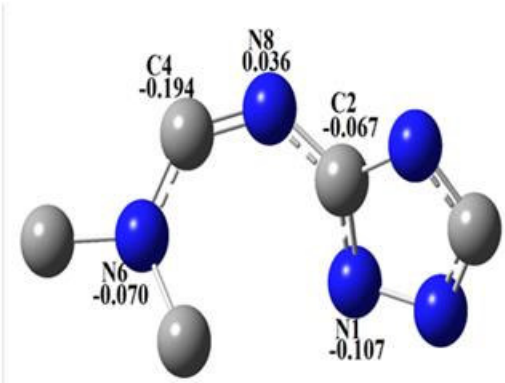

L_3

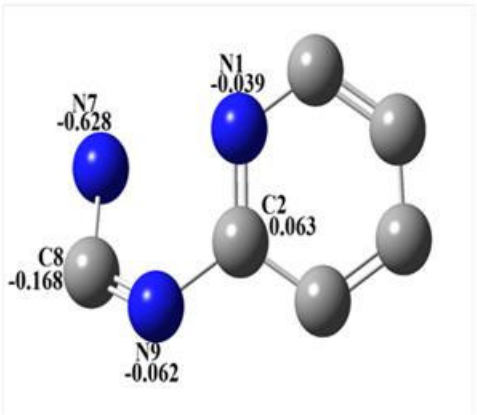

L_4

L_1: N'-(benzothiazol-2-yl)-N, N-dimethylformamidine
L_2: (1H-benzoimidazol-2-yl)-N, dimethylformamidine
L_3: N, N-dimethyl-N'-(2H-1, 2, 4-triazol-3-yl) formamidine
L_4: (Z)-N'-(pyridin-2-yl) formamidine

Scheme 1: Optimized molecular structure of formamidine ligands, Carbon (grey), Nitrogen (blue), Sulfur (yellow), Hydrogen atoms are omitted for simplicity.

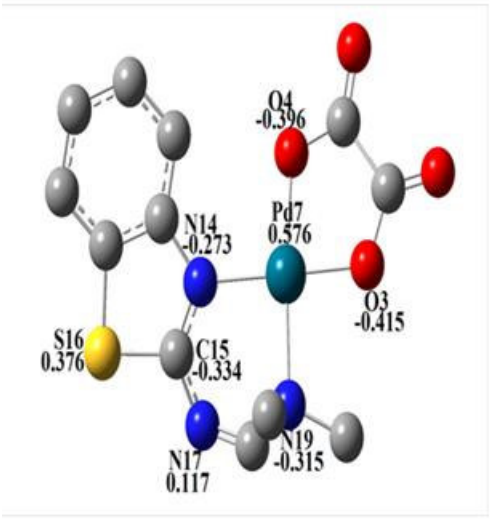

Complex (**1**)

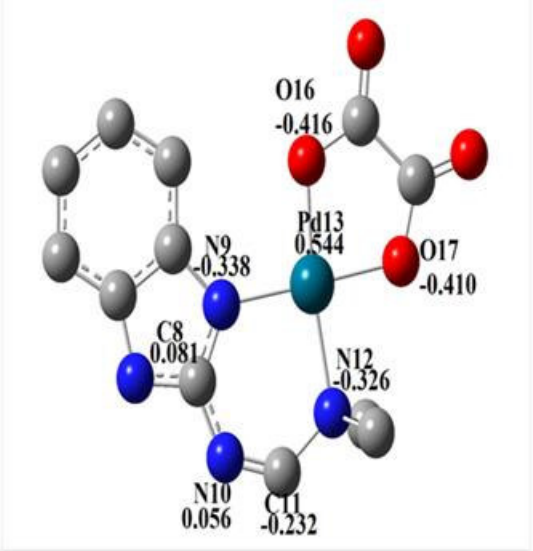

Complex (**2**)

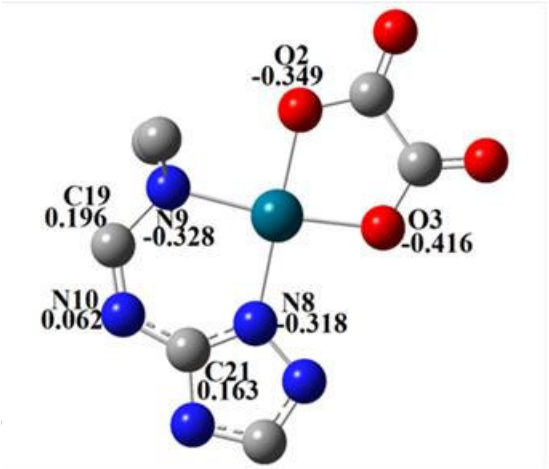

Complex (**3**)

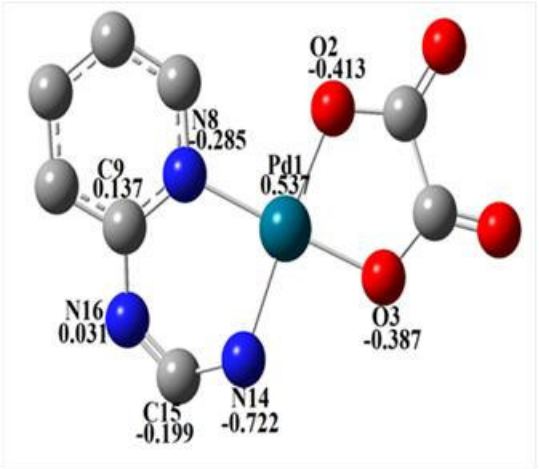

Complex (**4**)

Scheme 2. Optimized molecular structure and atomic charges of prepared Pd(II) oxalate complexes; by (Gaussian 09W software). Carbon (gray), Nitrogen (blue), Sulfur (yellow), Oxygen (red), and Palladium (green). Hydrogen atoms are omitted for simplicity.

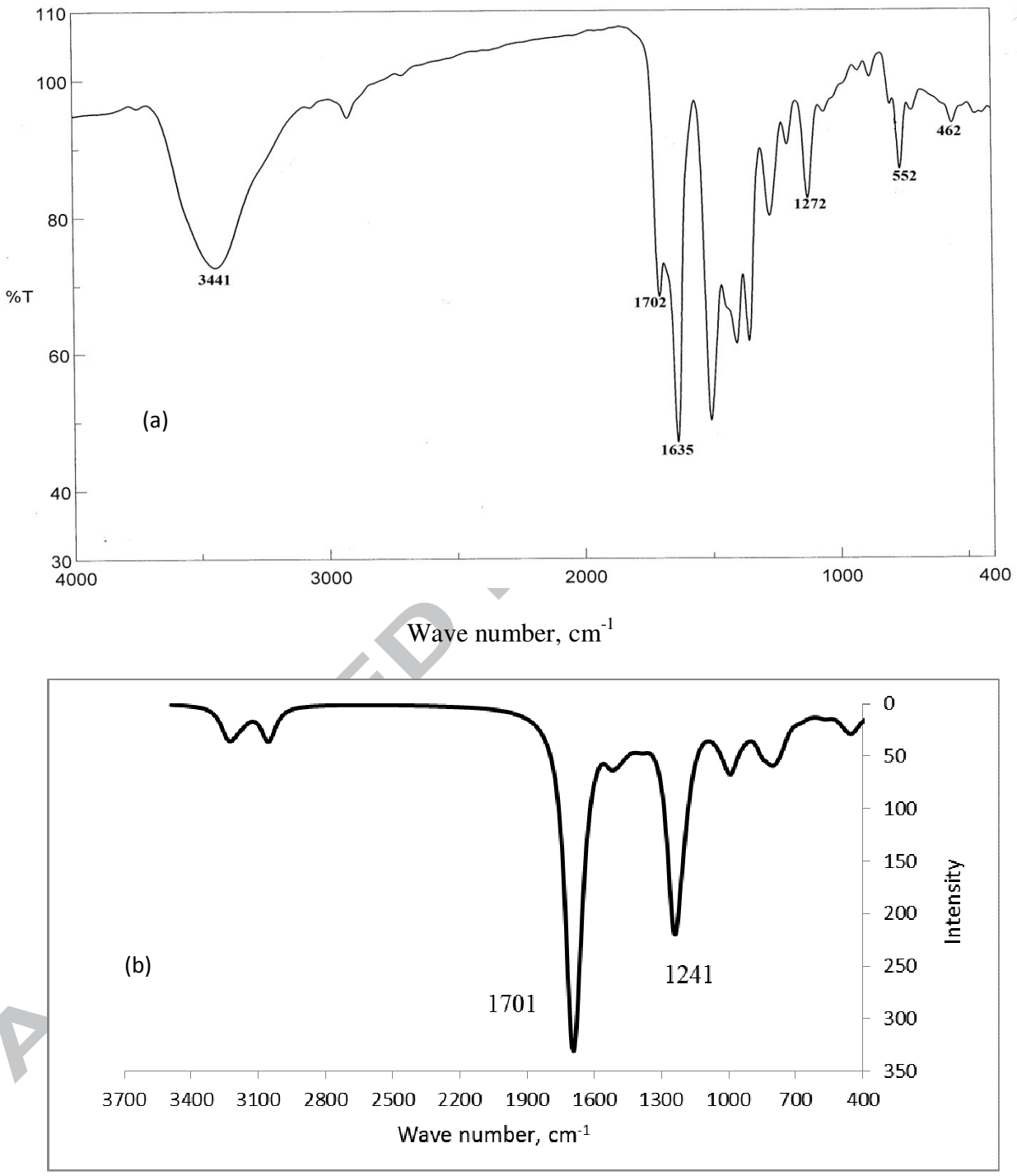

Fig. 1. IR spectra of Complex 1 experimental (a) and calculated (b).

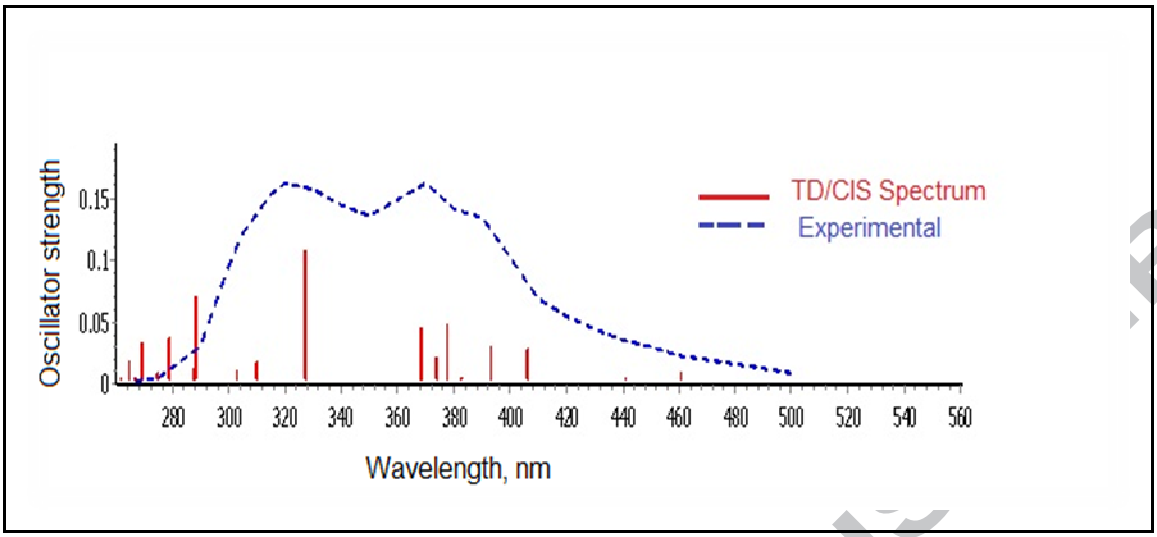

Fig. 2. The UV-visible spectra of complex 1 experimental (blue), and calculated (red).

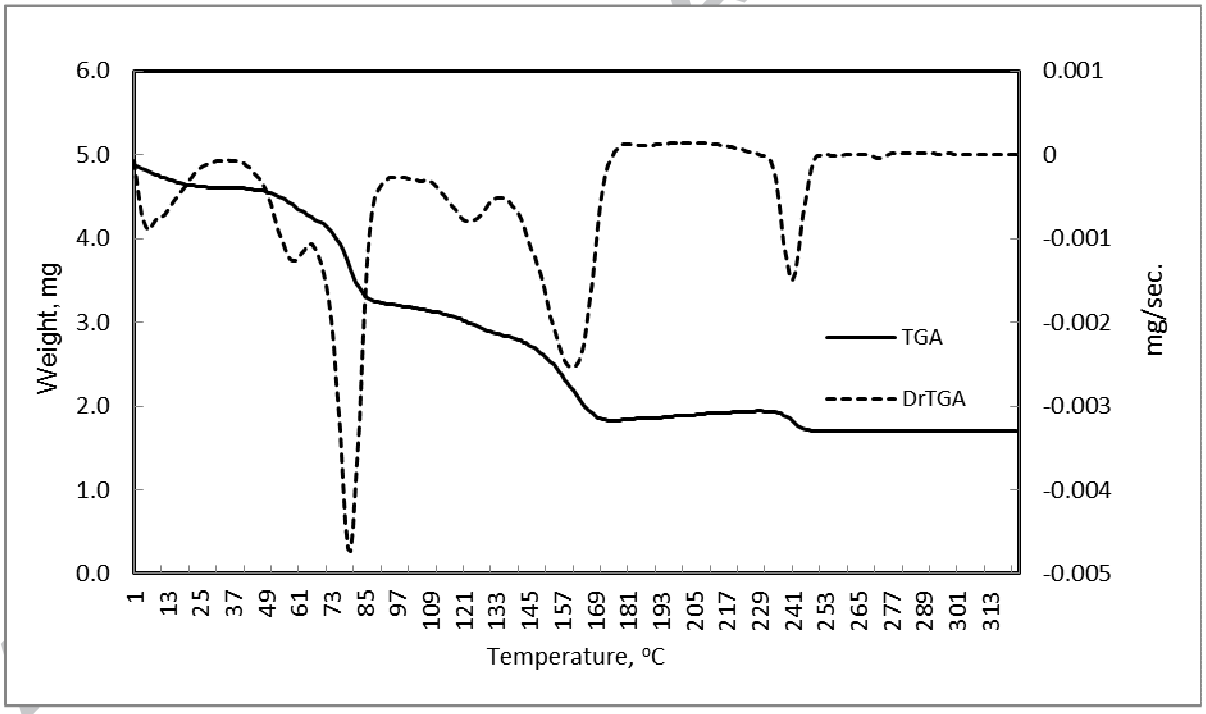

Fig. 3. The thermogram of complex (**3**)

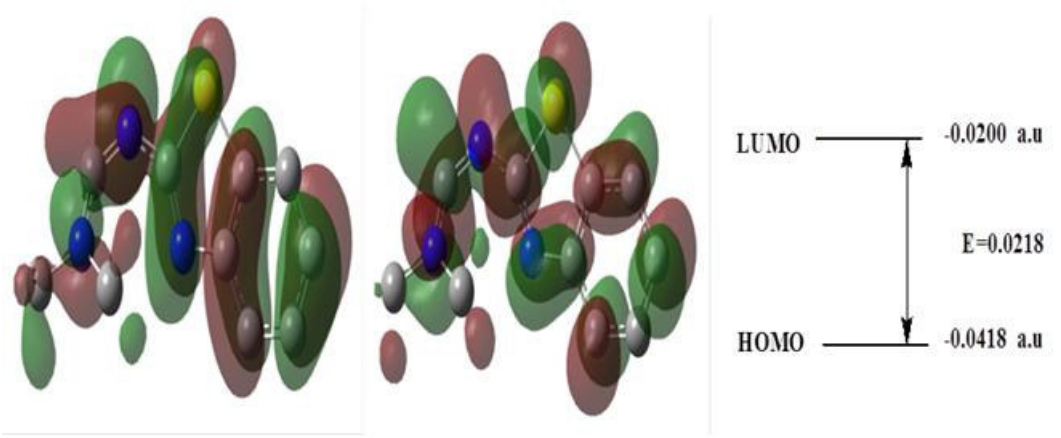

L_1 **HOMO**-Molecular Orbitals L_1-**LUMO**- Molecular Orbitals

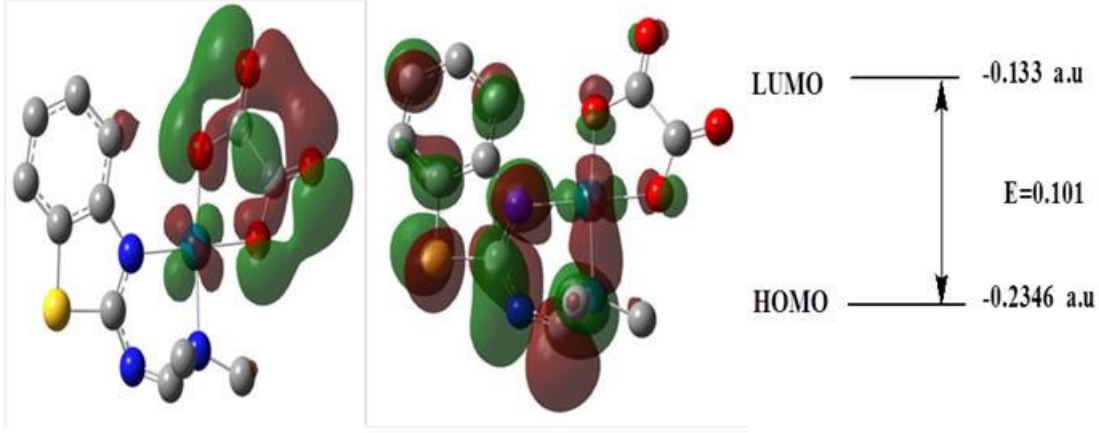

Complex (1) HOMO-Molecular Orbitals **Complex (1) LUMO**- Molecular Orbitals

Fig. 4. HOMO and LUMO orbitals and energy gap of L_1 and Complex 1, Red regions (negative) and green regions (positive).

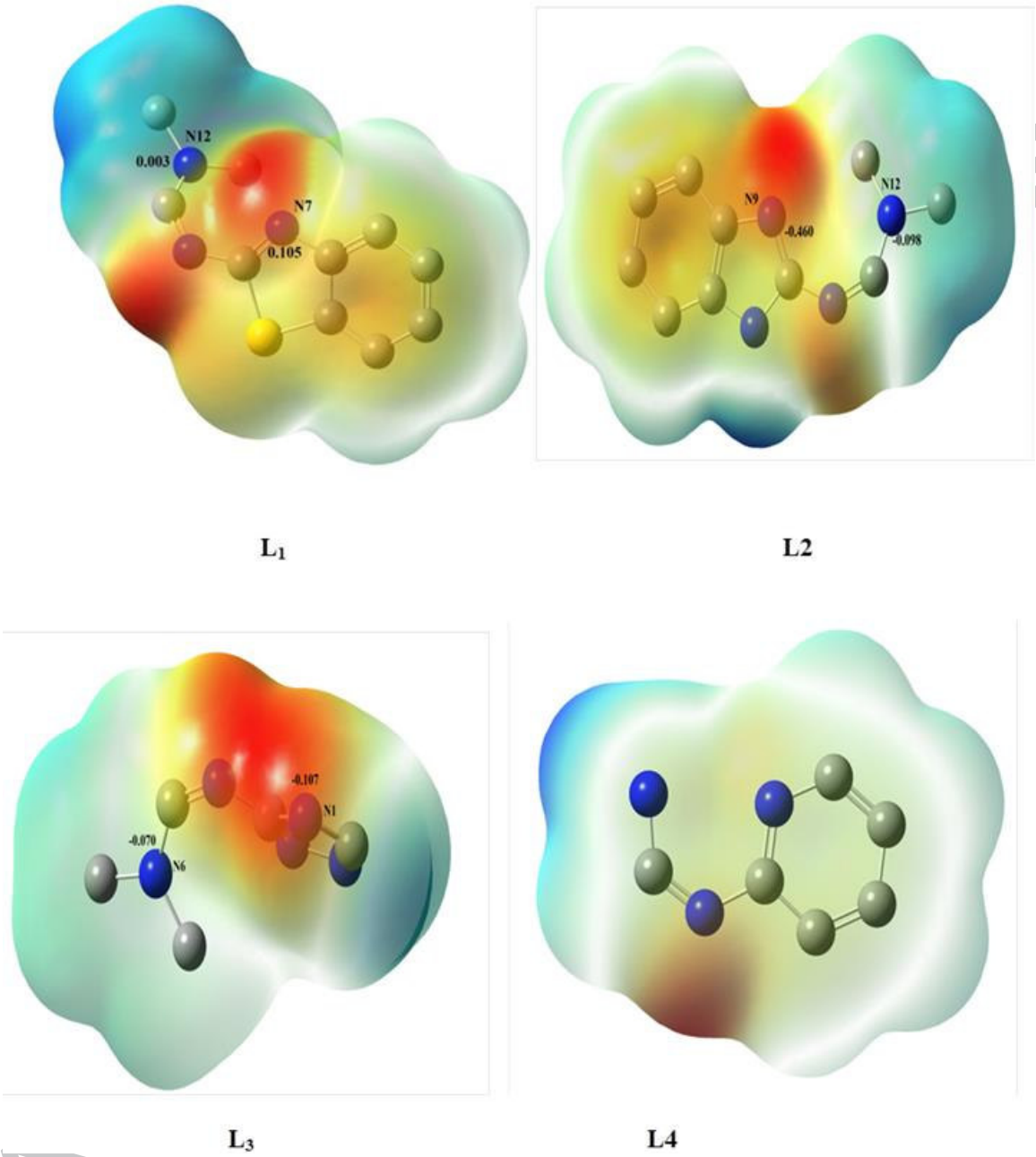

Fig. 5. Total Density of Electron Distributions of formamidine ligands. Hydrogen atoms are omitted for simplicity.

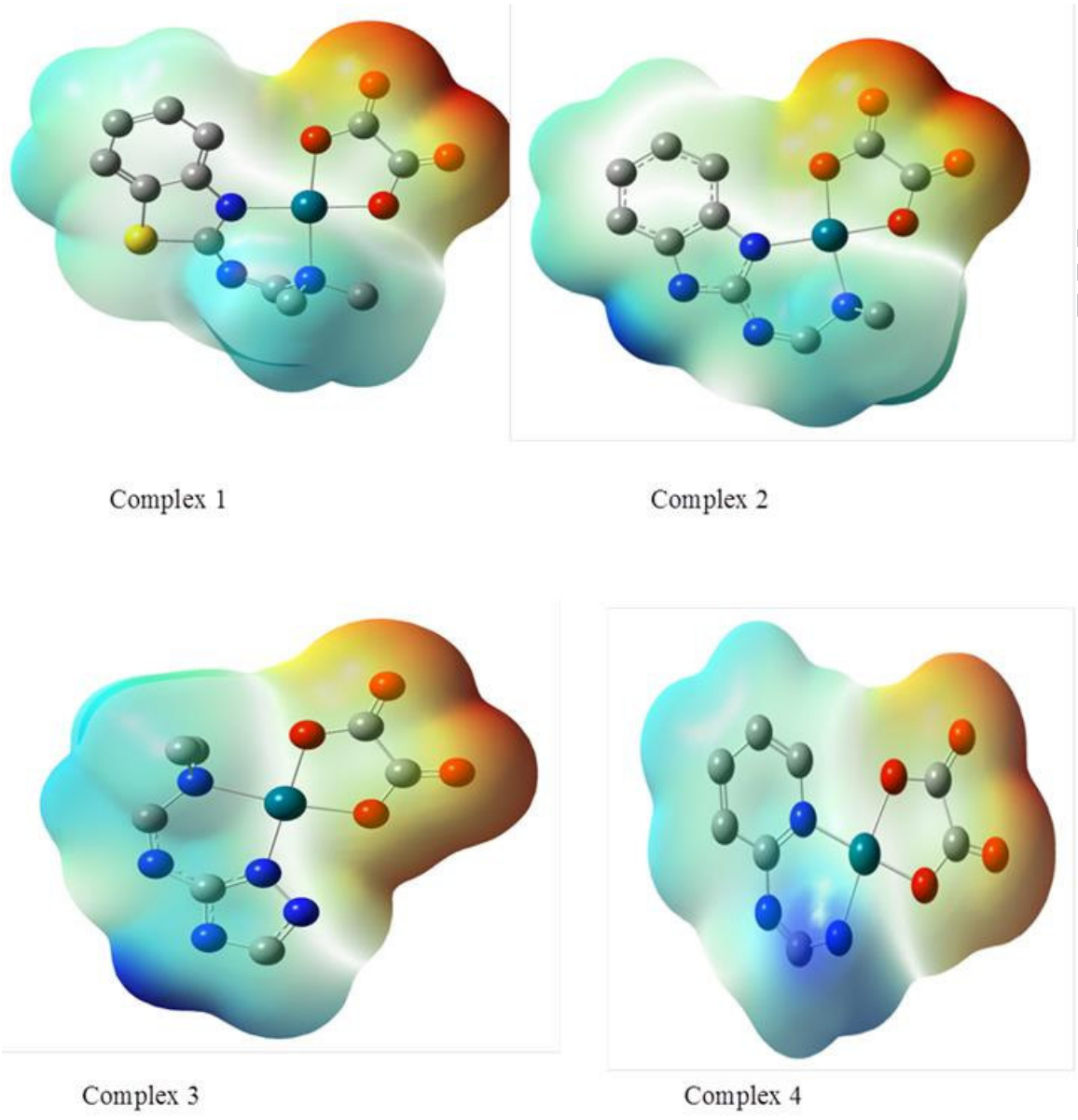

Fig. 6. Total Density of Electron Distributions of Pd(II) complexes. Hydrogen atoms are omitted for simplicity.

Table 1

The analytical, physical and spectroscopic data of the ligands and Pd(II) complexe

Complexes	Molar mass	color	Solubility	m.p	UV-Vis absorption peaks (nm)	assignment
$[Pd(L_1)ox].H_2O$	417.73	Pale yellow	DMSO	220	310-320 330-345 415	π-π* n-π* MLCT
$[Pd(L_2)ox].H_2O$	400.68	yellow	DMSO	245	310-325 330-350 420	π-π* n-π* MLCT
$[Pd(L_3)ox].4H_2O$	405.66	orange	Insoluble	226	Insoluble	
$[Pd(L_4)ox].$ $5/2H_2O$	360.62	yellow	DMSO	180	320-340 380-395 425	π-π* n-π* MLCT

Table 2

Most characteristic calculated and observed vibrational frequencies cm^{-1} for Pd(II) complexes

Compound	Obs.	Calc.	Relative error	Assignment
L_1	1618	1613	-0.30	υ(C=N) imin
	1276	1297	1.60	υ(C-N)
L_2	1632	1607	-1.50	υ(C=N) imin
	1274	1291	1.20	υ(C-N)
L_3	1634	1730	5,80	υ(C=N) imin
	1261	1245	-1.20	υ(C-N)
L_4	1631	1642	0.60	υ(C=N) imin
	1294	1273	-1.60	υ(C-N)
$[Pd(L_1)ox].H_2O$	3441	-		υ(O-H) Hydrated
	1635	1678	2.60	υ(C=N) imin
	1272	1262	0.70	υ(C-N)
	1702	1701	-0.05	υ(C=O) oxalate
	757	765	1.00	υ(M-O)
	462	433	-6.20	υ(M-N)
$[Pd(L_2)ox].H_2O$	3446	-		υ(O-H) Hydrated
	1641	1710	4.20	υ(C=N) imin
	1283	1265	-1.40	υ(C-N)
	1699	1697	-0.10	υ(C=O) oxalate
	752	767	1.19	υ(M-O)
	452	442	-2.20	υ(M-N)
$[Pd(L_3)ox].4H_2O$	3426	-		υ(O-H) Hydrated
	1636	1706	4.20	υ(C=N) imin
	1381	1391	0.70	υ(C-N)

	1704	1698	-0.30	υ(C=O) oxalate
	722	769	6.10	υ(M-O)
	450	470	4.40	υ(M-N)
$[Pd(L_4)ox].5/2H_2O$	3415	-		υ(O-H) Hydrated
	1627	1722	5.50	υ(C=N) imin
	1298	1304	0.40	υ(C-N)
	1712	1701	-0.60	υ(C=O) oxalate
	799	772	-3.40	υ(M-O)
	691	670	-3.10	υ(M-N)

Relative error = {(calc –exp)/exp} x 100

Table 3

Important mass data of Pd(II) complexes

complex	Molar mass	Important mass fragmentations (m/z) values
$[Pd(L_1)ox].H_2O$(**1**)	417.73	**420** (M+2), **400** (M-H_2O), **330** (M-C_2O_4)**, 213** (M-L_1), **205** (L_1), **121** PdO, Pd isotopes **103, 105, 107,108,109**
$[Pd(L_2)ox].H_2O$(**2**)	400.68	**400** (M), **382** (M-H_2O), **330** (M-(CO_2, CO)), **213** (M-L_2), **191** (L_2), **121** (PdO), Pd isotopes **107, 109, 110**
$[Pd(L_3)ox].4H_2O$(**3**)	405.66	**408** (M+2), **387** (M-H_2O), **351** (M-3H_2O), **333** (M-4H_2O), **317** (M-C_2O_4)**, 265** (M-L_3), **138** (L_3), **122** (PdO), Pd isotopes **110**, **111**
$[Pd(L_4)ox].5/2H_2O$(**4**)	360.62	**361 (M)**, **343 (M-**H_2O), **316 (M-5/2**H_2O)**, 272** (M-C_2O_4),

		238 (M-L_4), **121** (L_4), Pd isotopes **105, 107, 108, 110**

Table 4

Computed excitation energies (a.u), percent contribution from Pd, ox, ligands, and main character of some frontier orbitals of the studied complexes obtained from the calculations

Complex	Orb.[a]	Type[b]	Energy (a.u)	ox	Ligand	Pd	Main character
[Pd(L_1)ox)].H_2O (80)	H	O	-0.23	94%	1%	5%	ox(π)
(79)	H-1	O	-0.26	57%	14%	29%	ox(π), Pd(t_2g)
(78)	H-2	O	-0.26	57%	10%	33%	ox(π), Pd(t_2g)
(77)	H-3	O	-0.27	34%	4%	61%	ox(π), Pd(eg)

(76)	H-4	O	-0.27	68%	18%	14%	$L_1(\pi)$, ox(π)
(81)	L	V	-0.13	4%	90%	7%	$L_1(\pi^*)$
(82)	L+1	V	-0.09	26%	26%	48%	Pd(eg), $L_1(\pi^*)$
(83)	L+2	V	-0.04	10%	86%	4%	$L_1(\pi^*)$
(84)	L+3	V	-0.04	16%	83%	1%	ox(π^*), $L_1(\pi^*)$
(85)	L+4	V	-0.03	71%	29%	1%	$L_1(\pi^*)$
[Pd(L_2)ox)].H_2O							
(81)	H	O	-0.22	94%	1%	5%	ox(π)
(80)	H-1	O	-0.24	51%	18%	31%	ox(π), Pd(t_2g),
(79)	H-2	O	-0.25	59%	7%	34%	ox(π), Pd(t_2g)
(78)	H-3	O	-0.26	35%	3%	62%	ox(π), Pd(eg)
(77)	H-4	O	-0.26	77%	7%	16%	ox(π), Pd(eg)
(82)	L	V	-0.11	0%	98%	2%	$L_2(\pi^*)$
(83)	L+1	V	-0.07	27%	18%	55%	Pd(eg), ox(π^*)
(84)	L+2	V	-0.03	27%	70%	3%	$L_2(\pi^*)$, ox(π^*)
(85)	L+3	V	-0.03	69%	30%	1%	ox(π^*), $L_2(\pi^*)$
(86)	L+4	V	-0.02	0%	100%	0%	$L_2(\pi)$
[Pd(L_4)ox)].5/2H_2O							
(63)	H	O	-0.23	95%	1%	4%	ox(π)
(62)	H-1	O	-0.25	70%	2%	28%	ox(π), Pd(t_2g)
(61)	H-2	O	-0.26	63%	3%	34%	ox(π), Pd(t_2g)
(60)	H-3	O	-0.27	82%	6%	12%	ox(π), Pd(eg)
(59)	H-4	O	-0.28	36%	2%	62%	Pd(eg), ox(π)
(64)	L	V	-0.12	2%	93%	5%	$L_4(\pi^*)$
(65)	L+1	V	-0.09	12%	65%	22%	$L_4(\pi^*)$, Pd(t_2g), Pd(eg)
(66)	L+2	V	-0.07	14%	57%	29%	Pd(eg), Pd(t_2g), $L_4(\pi^*)$
(67)	L+3	V	-0.04	55%	37%	8%	$L_4(\pi^*)$, ox(π^*)

(68)	L+4	V	-0.03	42%	53%	5%	$L_4(\pi^*)$, $L_4(\pi^*)$

[a] H and L represent the HOMO and LUMO, respectively. H+n indicates the nth molecular orbital above the HOMO and L-n indicates the nth molecular orbital below the LUMO.
[b] V, and O represent unoccupied (virtual), and doubly occupied molecular orbitals, respectively.

Table 5
Thermogravimetric analytical data for decomposition of palladium(II) complexes

Complex	Molar mass	TG range (K)	DTA $_{max}$ (K)	Mass loss found (cal. %)	Assignment of the removed species	Metallic residue found (cal. %)
$[Pd(L_1)ox].H_2O$	417.73	374-530 542-584 611-1085	501 565 1042	60.56; (59.76) 10.13; (10.47) 4.09 ; (3.81)	$[H_2O,L_1,CO]$ CO_2 ½ O_2	Pd 25.22, (25.47)
$[Pd(L_2)ox].H_2O$	400.68	312-448 448-543 543-669 669-1046	319 499 630 1030	4.39; (4.50) 14.31; (14.0) 50.53; (50.07) 4.64; (4.00)	H_2O 2CO $[L_2,O]$ ½ O_2	Pd 26.13, (26.55)
$[Pd(L_3)ox].4H_2O$	405.66	343-497 479-558 558-677 677-800 1006-1036	479 540 671 783 1024	8.64; (8.82) 19.77; (19.60) 7.01; (6.86) 33.70; (34.26) 3.91; (3.92)	$2H_2O$ $[2H_2O,CO_2]$ CO L_3 ½ O_2	Pd 26.97, (26.23)
$[Pd(L_4)ox].$ $5/2H_2O$	360.62	315-408 408-460 460-567 567-1026	406 439 563 995	4.66; (4.95) 56.39; (56.47) 4.38; (4.40) 4.27; (4.40)	H_2O $[3/2H_2O,L_4,2CO]$ ½ O_2 ½ O_2	Pd 30.30, (29.51)

Table 6

Thermodynamic data of the thermal decompositions of Pd(II) complexes

Complex	Decomposition temperature (K)	ΔE/ KJ mol^{-1}	R^2	ΔS/ J K^{-1} mol^{-1}	ΔH/ KJ mol^{-1}	ΔG/ KJ mol^{-1}
$[Pd(L_1)ox].H_2O$	374-530 542 -584 611-1085	217 203 21	0.86 0.98 0.86	76 102 -271	211 198 12	162 140 295
		441		**-93**	**421**	**597**
$[Pd(L_2)ox].H_2O$	312-448 448-543 543-669 669-1046	217 106 146 17	0.89 0.98 0.95 0.85	76 -48 -26 -270	211 102 141 8	162 126 157 187
		486		**-268**	**462**	**732**
$[Pd(L_3)ox].4H_2O$	343-497 479-558 558 -677 677-800 1006-1036	217 200 92 179	0.88 0.98 0.96 0.98 0.99	76 116 -127 -34	211 196 86 172	162 133 172 200
		688		**31**	**665**	**667**
$[Pd(L_4)ox].5/2H_2O$	315-408 408-460 460-567 567-1026	217 232 32 19	0.91 0.98 0.87 0.85	76 301 -213 -294	211 229 27 11	162 108 149 304
		500		**-130**	**478**	**723**

Table 7

Equilibrium geometric parameters bond lengths (Å), bond angles (°), dihedral angles (°), total energy, and total dipole moment of optimized Pd(II) complexes by using DFT/B3LYP/SDD set basis.

Bond Lengths ^{o} A		Bond Angles ^{o}	
[Pd(L_1)ox)].H_2O			
Pd(7)-O(3)	2.01	O(3)-Pd(7)O(4)	82.70
Pd(7)-O(4)	1.99	O(3)-Pd(7)-N(14)	96.64
Pd(7)-N(14)	2.09	O(4)-Pd(7)-N(19)	91.51
Pd(7)-N(19)	2.17	N(14)-Pd(7)-N(19)	89.11
		O(4)-Pd(7)-N(14)	179.18
		O(3)-Pd(7)-N(19)	173.95
[Pd(L_2)ox].H_2O			
Pd(13)-O(17)	2.00	O(16)Pd(13)-O(17)	83.18
Pd(13)-O(16)	2.01	N(9)Pd(13)-O(16)	95.62
Pd(13)-N(9)	2.04	N(12)Pd(13)-O(17)	88.21
Pd(13)-N(12)	2.14	N(9)Pd(13)-N(12)	92.97
		N(9)-Pd(13)-O(17)	178.80
		N(12)-Pd(13)-O(16)	171.40
[Pd(L_3)ox].$4H_2O$			
Pd(1)-O(3)	1.99	O(2)-Pd(1)-O(2)	83.87
Pd(1)-O(2)	1.99	O(2)-Pd(1)-N(8)	96.03
Pd(1)- N(8)	2.02	N(9)-Pd(1)-N(8)	91.90
Pd(1)- N(9)	2.15	O(3)-Pd(1)-N(9)	88.27
		N(8)-Pd(1)-O(3)	179.82
		N(9)-Pd(1)-O(2)	172.06
[Pd(L_4)ox].$5/2H_2O$			
Pd(1)-O(2)	2.00	O(2)-Pd(1)-O(3)	84.48
Pd(1)-O(3)	1.99	O(2)-Pd(1)-N(8)	93.98
Pd(1)- N(8)	2.01	N(8)-Pd(1)-N(14)	90.63
Pd(1)- N(14)	2.11	O(3)-Pd(1)-N(14)	90.86
		O(3)-Pd(1)-N(8)	178.41

Bond Lengths ^{o} A		Bond Angles ^{o}	
		O(2)-Pd(1)-N(14)	174.62

Table 8

Calculated physical parameters of ligands and complexes.

Compound	**D.M Debye**	**Total energy a.u**	**E_{LUMO}**	**E_{HOMO}**	**η**	**ΔE**
L_1	4.90	-949.99	-0.11	-0.42	0.16	0.31
L_2	3.66	-607.19	-0.03	-0.20	0.08	0.17
L_3	4.96	-469.57	-0.10	-0.21	0.05	0.11
L_4	1.93	-397.04	-0.03	-0.21	0.09	0.19
$[Pd(L_1)ox].H_2O$	13.97	-1455.04	-0.13	-0.23	0.05	0.10
$[Pd(L_2)ox].H_2O$	16.06	-1112.25	-0.12	-0.23	0.05	0.11
$[Pd(L_3)ox].4H_2O$	18.77	-974.62	-0.13	-0.22	0.05	0.09
$[Pd(L_4)ox].5/2H_2O$	15.76	-902.09	-0.12	-0.23	0.05	0.11

Table 9

Cytotoxicity activity of Pd(II) complexes (1, 2, and 4).

complexes	MCF-7 (breast carcinoma cell line)	HEPG2 (liver carcinoma cell line)	HCT-116 (Colon carcinoma cell line)
	Inhibition%	Inhibition%	Inhibition%
[Pd(L_1)ox].H_2O (1)	53.62	38.42	60.24
[Pd(L_2)ox].H_2O (2)	57.41	39.16	52.39
[Pd(L_4)ox].5/2H_2O (4)	38.92	31.58	47.13

Table 10

IC_{50} values the formamidine ligands and their Pd(II) complexes

Compound	IC_{50} µM			
	MCF-7	HCT-116	PC-3	HepG-2
L_1	0.024	0.025	-	0.040
L_2	0.050	0.115	-	0.051
L_3	0.168	0.150	-	0.222
L_4	0.011	0.012	-	0.006
[Pd(L_1)ox].H_2O (1)	0.040	0.043	0.042	-
[Pd(L_2)ox].H_2O (2)	0.057	0.083	0.094	-
[Pd(L_4)ox].5/2H_2O (4)	0.074	0.061	0.094	-
Ref. (Doxorubicin)	0.001	0.001	0.001	0.001

New formamidine ligands and their mixed ligand palladium(II) oxalate complexes: Synthesis, characterization in vitro cytotoxicity and DFT calculations

Ahmed A. Soliman[1*], Othman I. Alajrawy[1, 2], Fawzy A. Attabi[1] , Mohamed R. Shaaban[1] and W. Linert[3]

[1]Department of Chemistry, Faculty of Science, Cairo University, 12613 Giza, Egypt.
[2]College of Veterinary Medicine, Al-Anbar University, Fallujah, Iraq
[3]Institute of Applied Synthetic Chemistry, Vienna University of Technology, Getreidemarkt 9-163-AC, A-1060 Vienna, Austria.

Abstract

A series of new ternary palladium(II) complexes of the type $[Pd(L_{1-4})ox].xH_2O$ where L= formamidine ligands and ox=oxalate, were synthesized and characterized by elemental analyses, magnetic susceptibility, UV-Vis, infrared (*IR*) and mass spectroscopy and thermal analysis. The spectroscopic data indicated that the formamidine ligands act as bidentate N2 donors and the oxalate as O2 ligand.

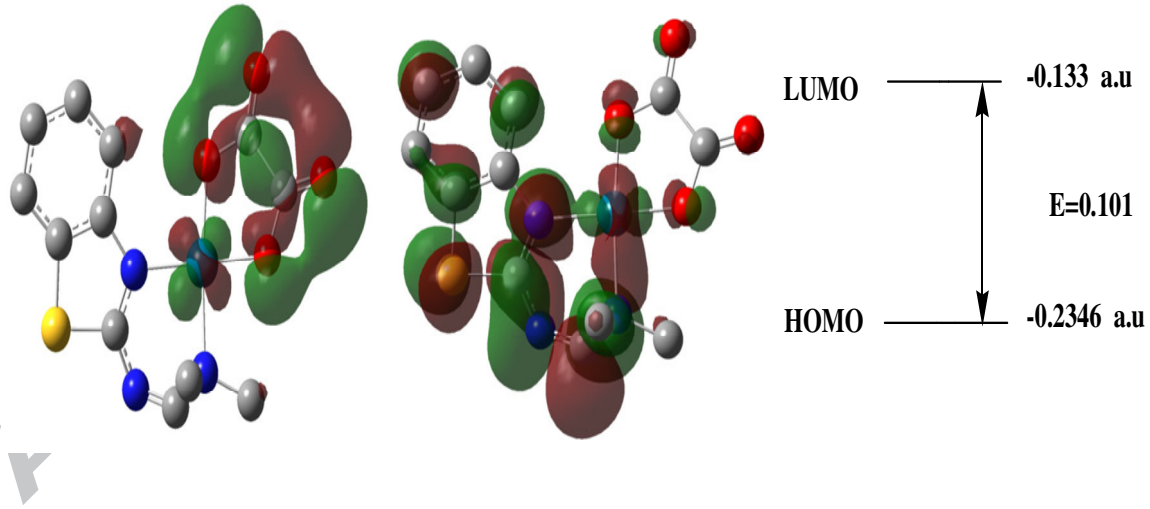

Complex (1) HOMO-Molecular Orbitals **Complex (1) LUMO-** Molecular Orbitals

Research Highlights

- New formamidine ligands were synthesized and characterized.
- Their mixed oxalate Pd(II) complexes were also synthesized and characterized.
- The structures are geometrically optimized and the computed vibrations and transition are compared with the experimental.
- The cytotoxicity of the ligands and complexes were tested with promising IC_{50} values.